FE-based Modeling of Gear-excited Vibrations and Vibroacoustic Transfer in Wind Turbine Drivetrains

Marc Zarnekow[1], Thomas Grätsch[1], Frank Ihlenburg[1]

[1] *Hochschule für Angewandte Wissenschaften Hamburg, 20099 Hamburg, Deutschland, Email: marc.zarnekow@haw-hamburg.de*

Introduction

Wind turbines near inhabited areas are no longer a rarity, often they are even difficult to avoid, in terms of available locations or wind and population distribution. For the protection of local residents, the wind turbines must therefore comply with strict emission requirements. A particularly critical feature of wind turbine noise are tonalities. Tonalities are narrow-banded peaks in the sound spectrum, which are considerably higher than the sound pressure at adjacent frequencies, see fig. 1. Tonalities are particularly stressful for the human ear and therefore heavily regulated [1].

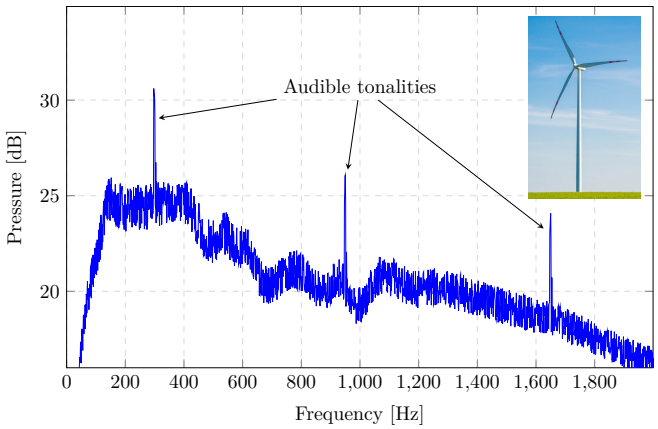

Figure 1: Typical far field sound spectrum of a wind turbine under operating conditions with three audible tonalities

Tonalities in the far field sound spectrum can be traced back to mechanical vibration sources inside the drive train, e.g. gearbox, generator or cooling fans. To investigate the transfer paths on which the sound propagate from vibration source to the various radiating structures (e.g. blades, cover or tower), this paper deals with the modeling and investigation of the vibro-acoustic transfer paths in a wind turbine under operating conditions. The resulting model shall be used to identify critical transfer paths and deduce targeted technical measures to reduce the sound radiation, in particular the tonalities.

Gear Excitation

Although the transfer paths are the main focus of this work, an adequate representation of the vibration source mechanism acting during operation is necessary for evaluating the transfer paths under operating conditions. Since the gearbox is an essential vibration source leading to tonality problems, it is important to determine the gear excitation. To achieve this, a spare modeling approach is implemented.

A correctly spaced and rigid gear connection with perfect involute teeth would produces no vibrations [2]. The fact that real gears still cause vibrations can basically be traced back to two main mechanisms [3]:

- geometrical deviations / errors regarding the perfect involute tooth shape
- time-varying mesh stiffness

The time-variable mesh stiffness leads to parameter-excited vibrations. A detailed finite element model is used to obtain this dominant source mechanism of gear excited vibrations. Therefore, the geometry of the investigated gear is modeled in the desired detail, where various relevant geometric properties can be considered (e.g. helical angle, profile modifications, manufacturing errors, etc.).

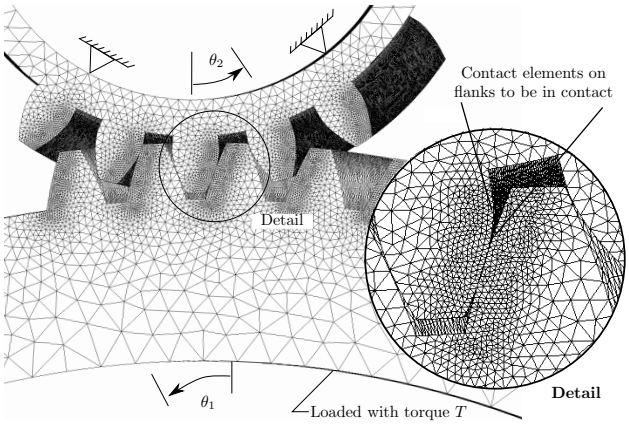

Figure 2: Schematic overview of the finite element setup to determine the mesh stiffness in a specific angular position within the mesh cycle

Fig. 2 shows the FE model. The driven gear is fixed in axial and radial direction and loaded with a torque T on its cylindrical face, while the driven gear is fixed in all directions on its cylindrical face. Both gears are connected via contact elements on the flanks with potential tooth contact, which are sufficiently finely meshed for this purpose. The model is simulated under static conditions.

Because of the finite mesh stiffness k_m, the driving gear rotates by an angle θ_1 under the load T. Since the rotation of the fixed driven gear θ_2 is zero, the mesh stiffness k_m for a specific angular position is calculated with

$$k_m = \frac{T}{r_{\mathrm{b},1}^2 \theta_1} \tag{1}$$

where $r_{\mathrm{b},1}$ denotes the base radius of the driving gear [4].

To determine the mesh stiffness variation over a mesh cycle, the previous described procedure is performed for a series of approx. 100 different angular positions within one mesh cycle. The results of the simulation are displayed in fig. 3.

For verification purpose the described procedure was applied to a literature example by Zhou [4] for a spur gear connection. The mesh stiffness, shown in fig. 3, shows a strict distinction between double teeth contact with relative high stiffness and single tooth contact with lower mesh stiffness. Our results are in good agreement to Zhou's results, whereas our model even better represents the theoretically expected and empirical measured rapid stiffness changes when the number of teeth in contact changes in spur gear connections [6].

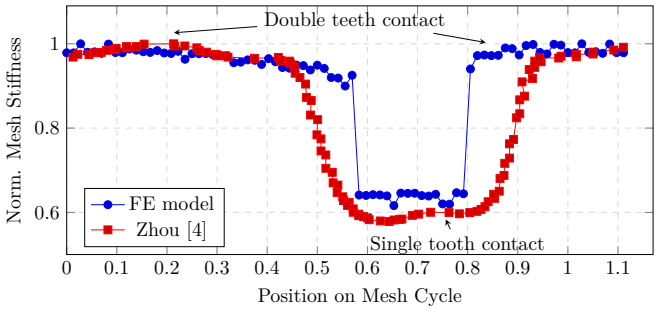

Figure 3: Varying mesh stiffness within a mesh cycle - Comparison of presented approach with results by Zhou [4]

To obtain the varying mesh stiffness of the investigated wind turbine gearbox, the presented approach is applied to the helical high speed gear stage. The results are shown in fig. 4. It can be seen that the higher contact ratio of the helical gears leads to a more complex angle and time-dependent variation of the mesh stiffness. Although the geometrical properties and resulting mesh stiffnesses are more complex for helical gears- the presented approach can be applied in the proposed way.

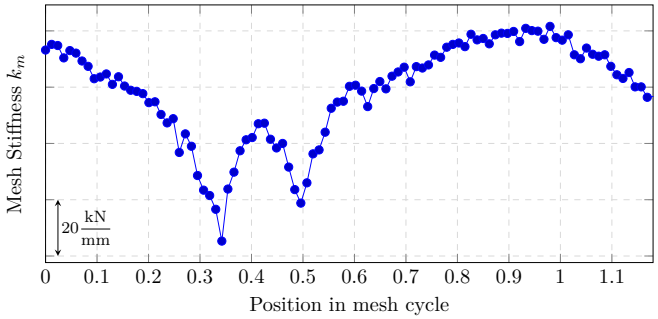

Figure 4: Varying mesh stiffness of a helical gear stage from a wind turbine gearbox

The gear excitation in the operating state is calculated by simulating the gearbox dynamics. For this purpose, the analytical model shown in fig. 5 is considered, in which the inertias are expressed as rigid disks, which are connected via mesh stiffness k_m and mesh damping c_m, see also [4]. The parameters k_G and c_G represent the stiffness and damping of the mounts and supporting structures (i.a. bearings, shafts).

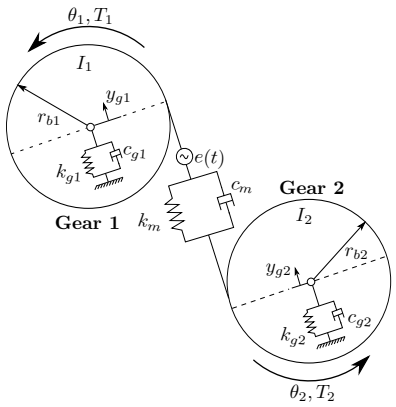

Figure 5: Analytical model to represent the gear dynamics

The meshing stiffness k_m is expressed with the values from the previous FE analyses as time-variable stiffness $k_m(t)$. The system in fig. 5 has four degrees of freedom, the rotational displacement θ and the translational displacement along the line-of-action y_G of each gear. By introducing the transmission error TE

$$TE = r_{b1}\theta_1 - r_{b2}\theta_2 \tag{2}$$

the two rotational degrees of freedom are reduced to one degree of freedom describing the relative linear displacement at the base radius r_b. The resulting system of three coupled ordinary differential equations is solved numerically in the time domain using the Runge-Kutta method. A Fourier transformation allows the calculation of the frequency spectrum of the dynamic gear excitation in the considered operating state. Fig. 16 shows the excitation spectrum in terms of the dynamic transmission error over the frequency, normalized to the mesh frequency of the high speed gear stage f_{mesh}, calculated for a wind turbine gearbox with 3 characteristic peaks.

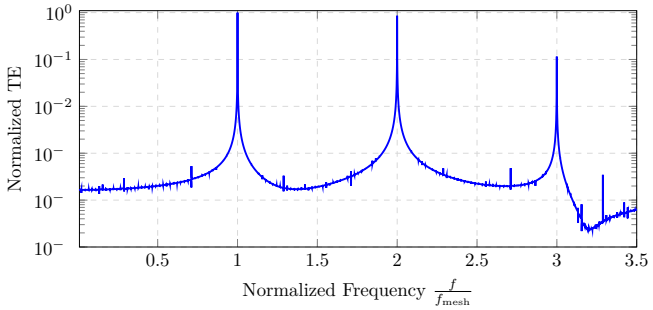

Figure 6: Frequency spectrum of the gear excitation in terms of the dynamic transmission error under operating conditions for a wind turbine gear box with 3 characteristic peaks

The obtained excitation spectrum represents the final result of the above presented approach to calculate the excitation spectrum by using an hybrid spare modeling approach.

Vibro-acoustic transfer paths

The investigation of the transfer behavior is based on a detailed dynamic finite element model, which is shown

in fig. 7. The model includes the components of the drive train as parts of the structure-borne sound path (i.e. gearbox, generator, rotor shaft, etc.) as well as the components which are considered to be the dominant radiating structures, such as rotor blades, tower, and nacelle housing.

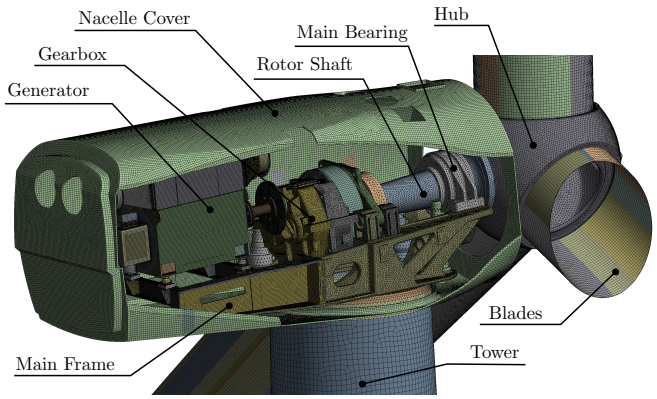

Figure 7: Detailed finite element model for structure-borne transfer path analysis of the wind turbine

The detailed FE model of the entire wind turbine consists of approx. 3.4 million FE nodes with approx. 12 million degrees of freedom. The model shall be analyzed in a frequency range from 0 to 2000 Hz with sufficiently fine frequency increments, in order to be able to resolve characteristic frequency peaks. The Craig-Bampton method is used for model order reduction.

As dynamic load, the transmission error of the considered gear stage is modeled as displacement excitation along the contact line. The response of the structure to a harmonic excitation with constant amplitude over the entire frequency range is calculated in the frequency domain. Fig. 8 shows a deformation response to a harmonic gear excitation with constant amplitude at meshing frequency. The frequency response of each response variable corresponds to a frequency-dependent transfer function $T(f)$.

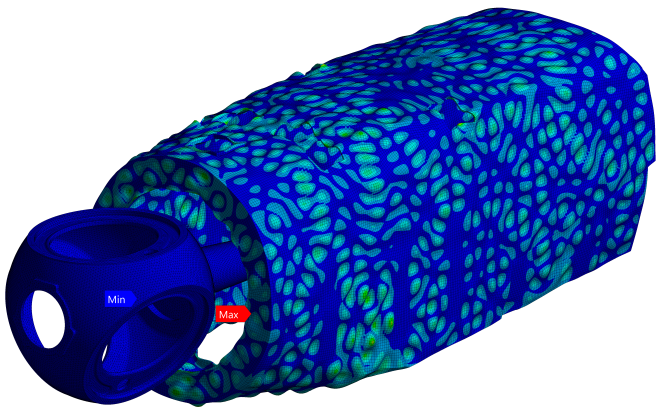

Figure 8: Calculated response shape of the drive train and nacelle cover to a harmonic gear excitation at mesh frequency

The calculation of the structural response under operating conditions is based on the assumption of linear behavior (non-linear behavior is linearized at the operating point). Under this assumption, the properties of linear systems are used to calculate the operational response. The operational response x_{Op} of an arbitrary response variable to one gear excitation source is calculated by combining the previously calculated gear excitation spectrum $TE(f)$ and the transfer function from the gear excitation source to the considered response variable $T(f)$ as follows:

$$x_{\mathrm{Op}} = T(f) \cdot TE(f) \tag{3}$$

This allows to calculate the response to one single source and to analyze and compare the response behavior. To evaluate the response to multiple sources, the responses to the single sources are computed separately as described above and the solutions are subsequently superimposed

$$x_{\mathrm{Op}} = \sum_{i=1}^{n} (T_{\mathrm{i}}(f) \cdot TE_{\mathrm{i}}(f)) \tag{4}$$

where n denotes the number of considered excitation sources (e.g. different gear stages of the same gearbox) and T_{i} and TE_{i} are defined as the transfer function to the considered response variable respective the excitation spectrum of the ith gear excitation source.

According to the presented procedure, the vibration responses under operational conditions of the entire system or of individual components with respect to different sources can be calculated and evaluated. Analogously, the frequency spectra of more complex response quantities can be determined, such as e.g. energies, structural intensities or the equivalent radiated power (ERP). Figure 9 shows the ERP spectra of different radiating surfaces, which can be used for panel contribution analysis to identify dominating and critical radiating structures.

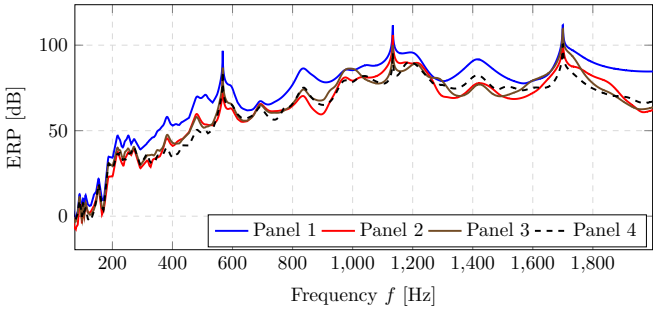

Figure 9: Calculated frequency spectra of the equivalent radiated power (ERP) under operating conditions for different radiating panels

Application

The computational models are used for the investigation of the various transfer paths within the drive train. As an example, the propagation of structural sound from gear vibrations (*source*) to the nacelle cover (*receiver*) is considered. According to [5], the major transfer paths in this case lead through the the torque arms (*TP 1*), through the main bearing (*TP 2*) and through the generator (*TP 3*)- see also Fig. 10. The equivalent radiated

power (ERP) is used as a measure of the response at the nacelle cover.

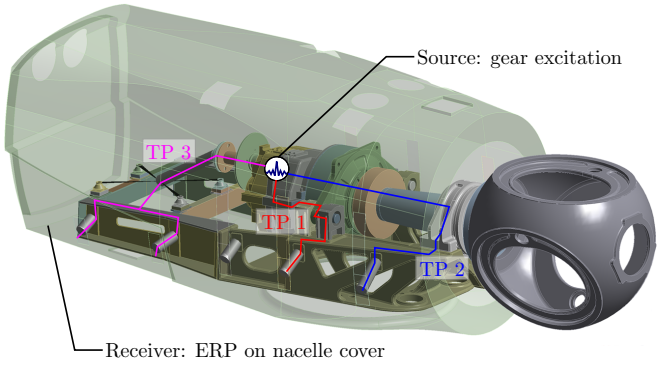

Figure 10: Application example to investigate the transmission of gear vibrations over three different structure-borne sound transfer paths

In order to evaluate the path contributions, three separate simulations for each of the transfer paths were carried out, blocking in every case two of the three major connections between the drive train and the nacelle cover. Thus, the contribution of each path to the radiated power on the nacelle cover can be quantitatively assessed and compared.

The comparison of the contributions of the individual paths is shown in figure 11. The results show that over almost the entire frequency range the radiation of the nacelle is dominated by the transfer via the *TP 3*. They also show that the transfer via the main bearing only makes a negligible contribution. It can also be seen, that the applied methodology confirms the initial assumption formulated for this example and enables the identification and quantification of critical transfer paths.

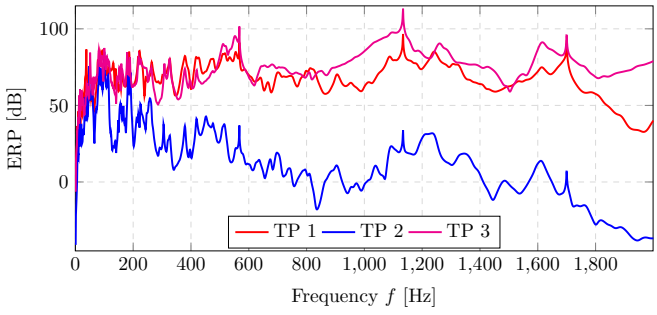

Figure 11: Contributions to the ERP level spectrum of the nacelle cover via the three different transfer paths

The comparison of the transfer path contributions is meaningful only if the blocking of the other transfer paths does not affect the global dynamic behavior. To evaluate this, the ERP results of the nacelle cover due to the isolated paths are superimposed and compared to the results calculated with a reference model (full transfer on all paths). The results are shown in fig. 12 and show very good agreement, especially at frequencies above $f = 200$ Hz. This confirms that the calculated single path contributions adequately represent the transfer behavior and allows meaningful evaluation of the different transfer paths.

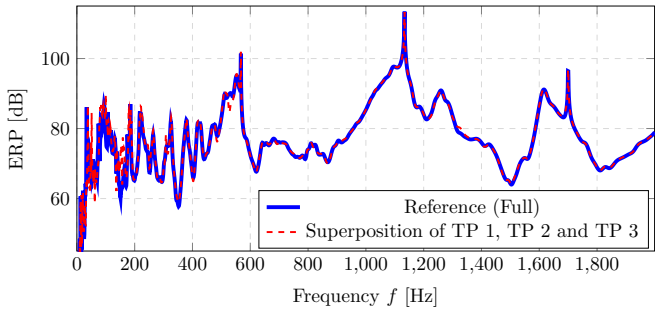

Figure 12: Frequency spectrum of equivalent radiated power (ERP) by the nacelle cover: The reference model with full transfer and the superposition of the results with isolated transfer paths show very good agreement

Conclusion & Outlook

A hybrid modeling approach for the calculation of transfer paths in wind turbines was presented. The approach combines a numerical-analytical model to determine the gear excitation with detailed dynamic FE models of the structure-borne sound path. By calculating transfer functions, the operating response is determined by using calculated excitation spectra. The application of the approach to the transfer path analysis of structural sound is illustrated in a computational example.

The next intended steps are an experimental validation of the modeling approach, a detailed investigation of the transfer paths inside a wind turbine and the extension of the model to also include airborne sound paths by FE acoustic models.

References

[1] Landström, U. et al.: Exposure levels, tonal components, and noise annoyance in working environments. In: Environment International 21.3 (1995), pp. 265-275

[2] Smith, J.D.: Gear Noise and Vibration, 2nd ed. Marcel Dekker, Inc., Cambridge, England, 2003

[3] Mark, D.: Analysis of the vibratory excitation of gear systems : Basic theory. In: J. Acoust. Soc. Am. 63 (1978), pp. 1409-1430.

[4] Zhou, J., Wenlei, S.: Vibration and Noise Radiation Characteristics of Gear Transmission System. In: J. Low Freq. Noise, Vib. Act. Control 30 (2014), pp. 485-502.

[5] Vanhollebeke, F.: Dynamic analysis of wind turbine gearbox components, Doctoral Thesis, 2015.

[6] Raghuwanshi, N.K., Parey, A., 2018. Experimental measurement of mesh stiffness by laser displacement sensor technique. Meas. J. Int. Meas. Confed. 128 (2018), pp. 63-70.